Nuclear Instruments and Methods in Physics Research B 272 (2012) 305–308

Contents lists available at ScienceDirect

Nuclear Instruments and Methods in Physics Research B

journal homepage: www.elsevier.com/locate/nimb

Photoluminescence studies on MBE grown Co-doped ZnO thin films fabricated through ion implantation and swift heavy ion irradiation

Basavaraj Angadi [a], Ravi Kumar [b], Dong-Hee Park [c], Ji-Won Choi [c], Won-Kook Choi [c,*]

[a] Department of Physics, Bangalore University, Bangalore-560 056, India
[b] Inter-University Accelerator Centre, Aruna Asaf Ali Marg, New-Delhi-110 067, India
[c] Optoelectronic Materials Center, Korea Institute of Science and Technology, Cheongryang, P.O. Box 131, Seoul 130-650, Republic of Korea

ARTICLE INFO

Article history:
Available online 2 February 2011

Keywords:
DMS
ZnO
Photoluminescence
Swift heavy ion

ABSTRACT

The temperature dependant photoluminescence of the Co-doped ZnO thin films, prepared by ion implantation on the MBE grown ZnO thin films followed by swift heavy ion irradiation, were investigated. The phenomenon of negative thermal quenching (NTQ), where the photoluminescence (PL) intensity increases with temperature, in contrast to the usual behavior of decrease in intensity with temperature, has been observed. The I_3 peak and the peaks (*a*, *b*, *c*, *d*, and *e*), corresponding to t_{2g} and e_g levels of the crystal field split Co *d* orbitals exhibit the NTQ behavior. The NTQ temperature range 35–45 K observed in un-doped ZnO shifts towards lower temperature with the Co doping. The increased number of dopant related and/or the vibrational/rotational resonance states with lower activation energies, from which the thermal excitation of the electrons takes place to the initial state of the PL transition, are responsible for the NTQ behavior.

1. Introduction

Recently ZnO, a II–VI semiconductor, has been emerged as a good candidate for high efficient UV/Blue emitting LED owing to its large exciton binding energy of 60 meV [1,2]. It has also been considered as a potential candidate for making oxide based dilute magnetic semiconductor (DMS) through doping with a small concentration of transition metal ions [3]. Among these, the Co-doped ZnO (Co:ZnO) is a well known DMS material with a ferromagnetic ordering at room temperature [3,4]. However, there are reports of difficulties in achieving the single phase Co:ZnO, due to the formation of Co clusters. A novel method of achieving a single phase Co:ZnO, through ion implantation followed by swift heavy ion (SHI) irradiation, was introduced and their magnetic and optical properties were studied in detail for their applications in spintronics devices [5,6]. The SHI irradiation, known for depositing large amount of energy to the lattice in a short span of time through electron–phonon interactions [7,8], help dissolving the Co clusters in Co:ZnO.

The thermal quenching phenomenon is commonly observed in the temperature dependant photoluminescence (PL) studies of many solids such as semiconductors and the ionic crystals [9,10]. This is mainly due to the temperature induced increase in the non-radiative recombination probability of electrons and holes. As a result, the intensity of the PL peaks decrease with increase in the measuring temperature. However, in contrast to this usual behavior some semiconducting materials such as GaAs [11,12] and ZnS [12,13] exhibit an increase in the PL intensity with an increment of temperature in some temperature range. This phenomenon is called 'Negative thermal quenching (NTQ)'. There have been various explanations for this unusual behavior [11,12,14]. Initially, Williams and Eyring [14] proposed analytical formulae for the observed phenomenon, which were not in agreement with some of the experimental results. Later, Bebb and co-workers [11,12] proposed a different mechanism for the NTQ observed in the (e-A^o) emission of GaAs, which was ascribed to the dissociation of the (D^o, X) system, which resulted in the ejection of a free electron into the conduction band. Recently, Shibata [15] suggested the principal mechanism of NTQ as a thermal excitation of electrons into the initial state of the PL transition from the eigen-states with smaller energy eigen-values.

The NTQ was also observed in single crystals, nanorods and bulk samples of un-doped ZnO and in Ga-doped ZnO thin films [16–18]. Meyer et al. [19] explained the NTQ behavior of I_{6B}/I_{8B} donor bound exciton PL peaks at 15–20 K in ZnO crystal, through fitting an analytical equation, in terms of the emergence of excited states involving B-valence band. In a similar way, Jung et al. [20] explained the enhancement of I_{10} peak intensity at 40–50 K in un-doped ZnO thin film grown by plasma-assisted MBE, in terms of both the thermal-

* Corresponding author. Tel.: +82 2 9585562.
E-mail addresses: brangadi@gmail.com (B. Angadi), ranade65@gmail.com (R. Kumar), pdmtime@kist.re.kr (D.-H. Park), jwchoi@kist.re.kr (J.-W. Choi), wkchoi@kist.re.kr (W.-K. Choi).

0168-583X/$ - see front matter © 2011 Published by Elsevier B.V.
doi:10.1016/j.nimb.2011.01.088

ization effect and the excitation to the vibronic/rotational resonance states or the involvement of B-valence band. Watanabe et al. [16] explained, through the analytical expression, the NTQ observed in the deep level emissions, donor–acceptor pair emissions and the bound excitonic emissions in the ZnO single crystals. Recently, He et al. [17] observed the NTQ in the green band of ZnO nanorods along with the remarkable increase in the life time and suggested the multiple trapping and de-trapping mechanism is responsible for the observed behavior. In our previous work [21], we presented the NTQ behavior observed in the un-doped and Ga-doped ZnO thin films deposited by the PA-MBE technique.

In this work, we are presenting the temperature dependant photoluminescence characteristics and NTQ behavior observed in Co-doped ZnO thin films prepared by ion implantation followed by swift heavy ion irradiation.

2. Experimental

The un-doped ZnO thin films of about 400 nm were deposited onto single crystal Alumina (0 0 0 1) substrates by the plasma assisted molecular beam epitaxy (PA-MBE). An elemental Knudsen cell was used as a Zn source of 6 N purity and was maintained at 355 °C during the deposition. Active oxygen species were generated and spread over the substrate through an rf plasma source activated at 450 W. The substrate temperature was maintained at 720 °C during the deposition and the chamber base pressure was kept below 2×10^{-9} torr. The details of the film growth and properties are given elsewhere [22]. For the preparation of Co-doped ZnO, the negative Co ions were implanted onto un-doped ZnO thin films using source of negative ions by cesium sputtering (SNICS) (2 MV Pelletron, NEC) with an energy of 80 keV and the fluence of 1×10^{16}–1×10^{17} ions/cm^2. Further, the Co-implanted ZnO thin films were irradiated at room temperature with 200 MeV Ag^{+15} ions with the fluence of 1×10^{12} ions/cm^2, using 15UD Tandem Accelerator at Inter-University Accelerator Centre (IUAC), New Delhi, India. The details are given elsewhere [5].

Photoluminescence studies were carried out on pure and Co-doped ZnO thin films in the temperature range of 10–300 K using He–Cd laser (λ = 325 nm) as an excitation source. The incident angle and laser power were fixed at 45° and 25 mW, respectively. The temperature was controlled using Lakeshore temperature controller (model 331) with the sensitivity of 50 mK.

3. Results and discussion

The NTQ behavior can be analyzed by studying the Arrhenius plot of the PL intensity. Fig. 1 shows the PL curves of un-doped ZnO taken at different temperatures, in which the dominant emission at 3.365 eV, assigned as I_3 peak, is clearly seen at all temperatures. The intensity of this I_3 peak, corresponding to the donor bound excitons [23], is considered for the NTQ analysis. The inset of Fig. 1 shows the Arrhenius plot of NTQ characteristics of I_3 peak for the un-doped ZnO thin films. We can see from the figure that the PL intensity decreases with the increase in the measuring temperature up to 35 K and then it starts to increase and shows a peak at 45 K and after that it again starts to decrease continuously for the higher temperatures. The characteristic NTQ behavior is observed in the temperature range 35–45 K. This is in agreement with our earlier results of NTQ behavior observed in the temperature range 30–50 K for un-doped ZnO thin films [20], however, the temperature range is higher when compared to the results (10–20 K) of Watanabe et al. [16] for ZnO single crystals.

Fig. 2 shows the PL curves of 2×10^{16} ions/cm^2 Co-implanted ZnO thin films taken at different temperatures. The curves clearly show the appearance of three peaks (*a*, *b*, and *c*) and two broad

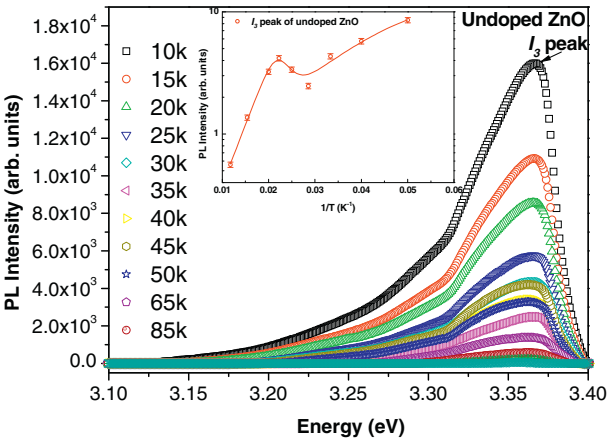

Fig. 1. The temperature dependant PL curves for un-doped ZnO thin film. The inset show NTQ characteristics of the I_3 peak of the same film.

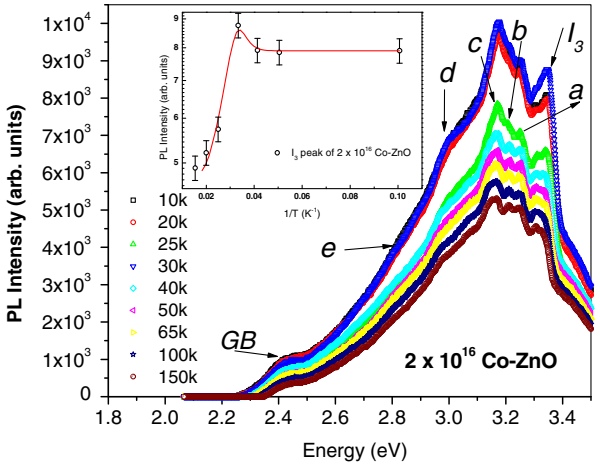

Fig. 2. The temperature dependant PL curves for 2×10^{16} ions/cm^2 Co-implanted and SHI irradiated ZnO thin film. The inset show the NTQ characteristics of the I_3 peak of the same film.

shoulders (*d* and *e*) along with the I_3 peak at 3.247, 3.211, and 3.169 eV, and at 2.975 and 2.815 eV, respectively. The new peaks are designated as t_{2g} (*a*, *b*, and *c*) and e_g (*d* and *e*) levels of crystal field split Co *d* orbitals in ZnO matrix [6]. This crystal field splitting corresponds to the tetrahedral symmetry of Co ions in Co^{2+} state (d^7), as reported by Wi et al. [24] through photoemission and X-ray absorption spectroscopy. The separation between the *a*, *b*, and *c* peaks (t_{2g} splitting) is observed to be 34 meV and that of *d* and *e* shoulders (e_g splitting) is 160 meV. The splitting between *c* and *d* (t_{2g} and e_g) is 194 meV. These values are in agreement with the local-spin-density approximation (LSDA) calculations by Park et al. [25]. The deep level emission at around 2.4 eV is also evident in Fig. 2; this is well known as green band (GB) in the literature and has been correlated to surface states such as oxygen vacancies.

The NTQ characteristics of the I_3 peak for the 2×10^{16} ions/cm^2 Co-implanted ZnO thin films is shown in the inset of Fig. 2. The figure shows the NTQ behavior in the temperature range 25–30 K ($k_BT \approx 2.1$–2.6 meV), this means a shift of about 15 K when compared to the un-doped ZnO film. From Fig. 2, it is clear (from the first three curves) that, not just the I_3 peak but all other peaks (*a*, *b*, *c*, *d*, and *e*) corresponding to the t_{2g} and e_g levels of the crystal field split Co *d* orbitals and the GB do exhibit the NTQ behavior in the same temperature range as that of the I_3 peak. The NTQ characteristics of the *a*, *b* and *c* peaks of the 2×10^{16} ions/cm^2 Co-im-

planted ZnO thin films are shown in the inset Fig. 3. All the three peaks exhibit the similar NTQ features in the temperature range 25–30 K, as that of the corresponding I_3 peak.

Fig. 4 shows the PL curves of 5×10^{16} ions/cm^2 Co-implanted ZnO thin films taken at different temperatures. The curves clearly show the relative increase in the intensity of the peaks corresponding to the t_{2g} and e_g levels compared to that of I_3 peak. This could be due to the relative increase in the population of corresponding t_{2g} and e_g levels compared to that of the I_3 peak. The inset of Fig. 4 shows the NTQ characteristics of the I_3 peak for the 5×10^{16} ions/cm^2 Co-implanted ZnO thin films. Though the NTQ behavior is not seen in the figure, but it appears that the NTQ temperature range shifts to temperatures less than 10 K, which is the lowest possible measurement temperature in our PL setup. The shift of NTQ temperature range with the Co doping can be clearly seen in Fig. 5, where the PL intensity of I_3 peak is plotted against temperature in the linear scale. It is also noteworthy that the position of I_3 peak shifts slightly towards lower energy with increasing Co doping concentration, whereas the positions of *a*, *b*, *c*, *d*, and *e* peaks are independent of Co doping.

The decrease in the NTQ temperature from the un-doped ZnO films to the Co-doped ZnO films with the increase in the Co doping concentrations is due to the possible increased addition of intermediate states and/or the vibrational/rotational resonance states with lower and lower activation energies. These levels contribute to the excitation of carriers, electrons, to the initial level of the PL transition. This is in addition to the existing impurity levels or the vibrational/rotational resonance states responsible for the NTQ behavior in the un-doped ZnO films.

The NTQ behavior can be understood in terms of the analytical function proposed by Shibata, [15] from which the activation energies associated with the intermediate states can be approximated,

$$\frac{I(T)}{I(0)} = \frac{1 + \sum_{q=1}^{w} D_q \exp\left(\frac{-E'_q}{(k_B T)}\right)}{1 + \sum_{j=1}^{m} C_j \exp\left(\frac{-E'_j}{(k_B T)}\right)} \quad (1)$$

where E'_q and E_j are the characteristic activation energies. We analyze our results assuming $w = 1$ and $m = 2$, which actually corresponds to one negative thermal quenching and two normal quenching behaviors over the entire temperature range of measurement. The solid curve in Fig. 3 and in the insets of Figs. 1, 2 and 4 corresponds to the non-linear curve fitting using Eq. (1) and the symbols represent the experimental data. The figures reveal a reasonable good fitting to the experimental data, implying the accurate determination of the parameters of Eq. (1). The most probable values obtained for E'_1, E_1 and E_2 are listed in Table 1 along with the nature of thermal quenching and the respective peak energy values. It can be seen from the table that, the activation energies 41–49 meV obtained for the E'_1 of I_3 peak at 3.365 eV of both un-doped and Co-doped ZnO films are in agreement with the value 42 meV (peak D at 3.3606 eV) of Watanabe et al. [16] and the 33 meV (peak in the spectral range 3.00–3.46 eV) of Hauser et al. [18]. However, with the Co doping the NTQ characteristics showed a considerable change, as can be seen in the nature of the curve and the estimated activation energies. In addition to the decrease in the NTQ temperature range, as mentioned before, noticeable changes

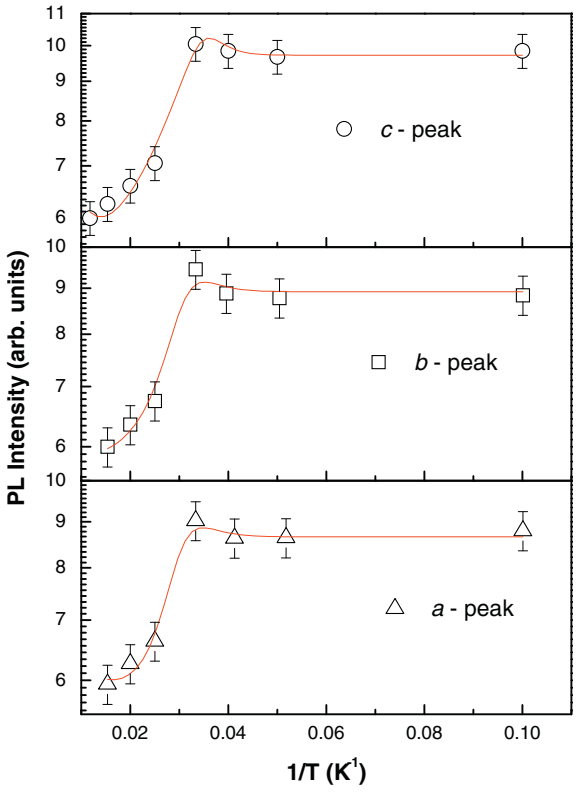

Fig. 3. The NTQ characteristics of the *a*, *b* and *c* peaks for 2×10^{16} ions/cm^2 Co-implanted and SHI irradiated ZnO thin film.

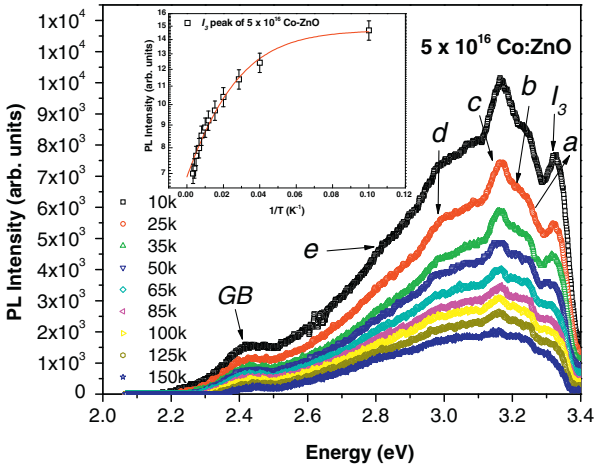

Fig. 4. The temperature dependant PL curves for 5×10^{16} ions/cm^2 Co-implanted and SHI irradiated ZnO thin films. The inset shows the NTQ characteristics of the I_3 peak of the same film.

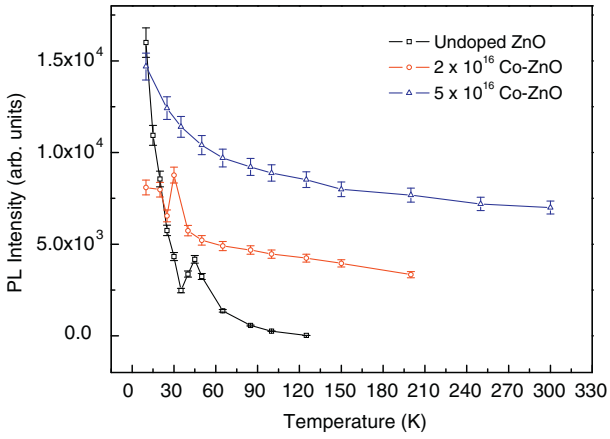

Fig. 5. Plots of PL intensity vs. temperature of I_3 peak for the un-doped and Co-implanted SHI irradiated ZnO thin films.

Table 1
Summary of the thermal quenching characteristics and the most probable values of E_1', E_1 and E_2, extracted by fitting the experimental data with Eq.(1).

Sample and peak	Peak energy (eV)	Thermal quenching	E_1'(meV)	E_1 (meV)	E_2 (meV)
Un-doped ZnO					
I_3 peak	3.365	Negative	49 ± 7	69 ± 6	7.2 ± 0.6
2×10^{16} Co–ZnO					
I_3 peak	3.344	Negative	41 ± 1	47 ± 1	54 ± 3
a-peak	3.247	Negative	35 ± 9	32 ± 3	31 ± 2
b-peak	3.211	Negative	35 ± 1	33 ± 2	32 ± 5
c-peak	3.169	Negative	40 ± 5	44 ± 5	48 ± 3
5×10^{16} Co–ZnO					
I_3 peak	3.327	Positive	–	–	4.2 ± 0.3

in the activation energies can be seen with the Co-doping. The activation energies obtained for the *a*, *b* and *c* peaks of the 2×10^{16} ions/cm^2 Co-implanted film were almost identical, of about 35 meV, except a slightly higher value 40 meV for the *c*-peak. This implies that the intermediate states responsible for the NTQ behavior populate these dopant related levels, which are the initial states of the respective PL transitions, at the same temperatures. The decrease in the NTQ temperature range with Co-doping corroborates with the decrease in the observed activation energies, as seen from Table 1. This might be due to the increased number of intermediate states with the lower and lower activation energies as mentioned before. For the 5×10^{16} ions/cm^2 Co-implanted film, as there was no NTQ behavior in the measured temperature range, the data was fitted only for E_2 corresponding to usual thermal quenching behavior. Similar normal thermal quenching behavior is evident for the other dopant related peaks (*a*, *b* and *c* peaks) and GB, as seen from Fig. 4. It is also noteworthy that the E_2 value corresponding to normal thermal quenching in un-doped ZnO, showed considerable change in 2×10^{16} ions/cm^2 Co-doped ZnO in which the NTQ was observed. However, the same value was restored in 5×10^{16} ions/cm^2 Co-doped ZnO where the NTQ was not observed in the measured temperature range.

4. Conclusions

The temperature dependant photoluminescence characteristics of the un-doped and the Co-doped ZnO thin films were investigated. The photoluminescence peak intensity of the I_3 peak and the *a*, *b* and *c* peaks, corresponding to the t_{2g} levels of the crystal field split Co *d* orbitals, exhibit the unusual negative thermal quenching behavior. The NTQ behavior observed in the temperature range 35–45 K, for the I_3 peak of the un-doped ZnO, shifts to lower temperature with Co-doping. The activation energies associated with the thermal quenching behavior were extracted by fitting the experimental results using an analytical function and are observed to be in agreement with the reported values. The shift in the NTQ temperature with Co-doping was ascribed to the increased contribution from the intermediate states which get activated at lower and lower temperatures.

Acknowledgements

The author, Won-Kook Choi, would like to appreciate the financial support from KIST Future Resource Program under the contract (2E21093). The author, BA would like to thank KIST for the visiting scientist fellowship.

References

[1] M.W. Cho, T. Minegishi, T. Suzuki, H. Suzuki, T. Yao, S.K. Hong, H. Ko, J. Electroceram. 17 (2006) 255.
[2] E. Gur, H. Asil, C. Coskun, S. Tuzemen, K. Meral, Y. Onganer, K. Serifoglu, Nucl. Instr. Meth. Phys. Res. B 266 (3) (2008) 2021.
[3] D.P. Norton, M.E. Overberg, S.J. Pearton, K. Pruessner, J.D. Budai, L.A. Boatner, M.F. Chisholm, J.S. Lee, Z.G. Khim, Y.D. Park, Appl. Phys. Lett. 83 (2003) 5488.
[4] N.A. Theodoropoulou, A.F. Hebard, D.P. Norton, J.D. Budai, L.A. Boatner, J.S. Lee, Z.G. Khim, Y.D. Park, M.E. Overberg, S.J. Pearton, R.G. Wilson, Solid State Electron. 47 (2003) 2231.
[5] Basavaraj Angadi, Y.S. Jung, Won-Kook Choi, Ravi Kumar, K. Jeong, S.W. Shin, J.H. Lee, J.H. Song, M. Wasi Khan, J.P. Srivastava, Appl. Phys. Lett. 88 (2006) 142502.
[6] Ravi Kumar, Fouran Singh, Basavaraj Angadi, Ji-Won Choi, Won-Kook Choi, Kwangho Jeong, J. Appl. Phys. 100 (2006) 113708.
[7] M. Toulemonde, S. Bouffard, F. Studer, Nucl. Instr. Meth. Phys. Res. B 91 (1994) 59.
[8] B. Angadi, V.M. Jali, M.T. Lagare, N.S. Kini, A.M. Umarji, Ravi Kumar, S.K. Arora, D. Kanjilal, Nucl. Instr. Meth. Phys. Res. B 187 (2002) 87.
[9] A.St. Amour, J.C. Sturn, Y. Lacroix, M.L.W. Thewalt, Appl. Phys. Lett. 65 (1994) 3344.
[10] S. Fukatsu, Y. Shiraki, J. Cryst. Growth 150 (1995) 1025.
[11] E.W. Williams, H.B. Bebb, in: R.K. Willardson, C. Beer (Eds.), Semiconductors and Semimetals, vol. 8, Sage, New York, 1972, p. 321.
[12] E.H. Bogardus, H.B. Bebb, Phys. Rev. 176 (1968) 993.
[13] T. Yokogawa, T. Taguchi, S. Fujita, M. Satoh, IEEE Trans. Electron. Devices 30 (1983) 271.
[14] F.E. Williams, H. Eyring, J. Chem. Phys. 15 (1947) 289.
[15] H. Shibata, JPN. J. Appl. Phys. 37 (1998) 550.
[16] M. Watanabe, M. Sakai, H. Shibata, C. Satou, S. Satou, T. Shibayama, H. Tampo, A. Yamada, K. Matsubara, K. Sakurai, S. Ishizuka, S. Niki, K. Maeda, I. Niikura, Physica B 376–377 (2006) 711.
[17] H. He, Z. Ye, S. Lin, B. Zhao, J. Huang, J. Phys. Chem. C 112 (2008) 14262.
[18] M. Hauser, A. Hepting, R. Hauschild, H. Zhou, J. Fallert, H. Kalt, C. Klingshrin, Appl. Phys. Lett. 92 (2008) 211105.
[19] B.K. Meyer, H. Alves, D.M. Hofmann, W. Kriegseis, D. Forster, F. Bertram, J. Christen, A. Hoffmann, M. Strburg, M. Dworzak, U. Haboeck, A.V. Rodina, Phys. Status Solidi B 241 (2004) 231.
[20] Y.S. Jung, W.K. Choi, O.V. Kononenko, G.N. Panin, J. Appl. Phys. 99 (2006) 13502.
[21] W.K. Choi, H.C. Park, B. Angadi, Y.S. Jung, J.W. Choi, J. Electroceram. 23 (2009) 331.
[22] Y.S. Jung, O. Kononenko, J.S. Kim, W.K. Choi, J. Cryst. Growth 274 (2005) 418.
[23] D.C. Reynolds, C.W. Litton, T.C. Collins, Phys. Rev. 140 (1965) A1726.
[24] S.C. Wi, J.-S. Kang, J.H. Kim, S.-B. Cho, B.J. Kim, S. Yoon, B.J. Suh, S.W. Han, K.H. Kim, J.H. Shim, B.I. Min, Appl. Phys. Lett. 84 (2004) 4233.
[25] M.S. Park, S.K. Kwon, B.I. Min, Phys. Rev. B 65 (2002) 161201.